

**Ablation of Multi-Wavelet Reentry:**

**Agreement between an Evolutionary Computational and a Conceptually Guided Strategy**

Shane Celis<sup>†</sup>, Nicholas Cheney\*, Margaret Eppstein<sup>†</sup>, Bryce Benson<sup>†</sup> and Peter Spector<sup>‡</sup>

<sup>†</sup>University of Vermont College of Engineering and Mathematics, \*Cornell University, <sup>‡</sup>University of Vermont College of Medicine

Corresponding Author:

Peter Spector

McClure 1 Cardiology,

111 Colchester Avenue,

Burlington, Vermont 05401

[peter.spector@uvm.edu](mailto:peter.spector@uvm.edu)

## **ABSTRACT**

Treatment of Multi-Wavelet Reentry (MWR) remains a challenge. Based upon the principles of propagation through excitable tissue, it has recently been proposed that MWR termination 1) requires circuit interruption; 2) circuit interruption requires linear ablations to connect to the tissue edge; 3) the probability of termination is proportional to the outer boundary length (including contiguous ablation) and inversely proportional to tissue area; and 4) ablation at sites of high rotor density have increased probability of termination. We describe an evolutionary computational search for MWR ablation strategies and examine whether the results conform to the principles above.

We used a covariance matrix adaptation evolutionary strategy to develop ablation lesion sets that minimize the ability of a two-dimensional sheet of tissue to maintain MWR in a computational model of cardiac tissue. The first generation was precluded from connecting to the tissue edge or quarantining cells. Fitness was defined as the average number of cell excitations in 2.5 seconds after ablation. Ten evolutionary trials were performed on two different types of tissue: 1) tissue with a homogeneous rotor distribution, and 2) tissue with a high rotor density patch.

As the evolutionary search proceeded, fitness improved. The percentage of ablation points contiguous with the tissue edge steadily increased, the total lesion length increased to the maximum allowable, and the tissue area was reduced through quarantine up to the maximum allowable. The result was an increased boundary length to tissue area ratio. Ablation density was uniform in the homogeneous tissue but higher in the high rotor density patch of the heterogeneous tissue.

An evolutionary strategy with no information about cardiac propagation nonetheless identified the principles of MWR ablation prescribed by a mechanistic ablation approach. This supports the validity of these principles and suggests that ablation of MWR in humans should be guided by the density of rotors and comprised of lesions contiguous with the tissue edge.

**KEYWORDS:** ablation, arrhythmia, catheter ablation, evolutionary computation, fibrillation, reentry

## **JOURNAL CLASSIFICATION:**

**10.030** Evolutionary Computing

**20.150** Biomedical Engineering

## **Introduction:**

Human atrial tissue constitutes a complex non-linear dynamic system. The atria are comprised of many millions of myocytes connected in a large syncytium. This system is capable of generating a staggeringly large number of potential activation patterns as excitation propagates through it. Under normal circumstances atrial activation proceeds in an organized and orderly fashion, with large coherent waves traversing across all cells and then extinguishing. Under pathologic conditions activation can propagate in continuous loops perpetually re-exciting the atria. Such is the case with multi-wavelet reentry (MWR), an abnormal heart rhythm affecting many millions of people worldwide (Calkins, Kuck et al.). The circuits that allow continuous propagation to persist in MWR are often dynamic, shifting in location overtime (Moe and Abildskov 1959). In MWR multiple independent circuits coexist and meander throughout the atria. In a therapeutic procedure called catheter ablation, one can create lines of scar tissue in the heart, across which propagation cannot occur, thereby altering the potential paths of activation (Jais, Hocini et al. 2004). Unfortunately ablation, which is extremely effective in the treatment of organized arrhythmias, has been much less effective for treatment of MWR (Calkins, Reynolds et al. 2009). The challenge for developing an effective MWR ablation strategy is to determine what *distribution* of linear scars would constrain atrial activation to allow only organized propagation – the “ablation problem”.

In a recent paper we elaborated a conceptual framework that delineates the requirements for perpetuation of reentrant arrhythmias regardless of the complexity of their circuitry (Spector 2012). This framework guided the development of an ablation strategy aimed at maximizing the probability of spontaneous termination of MWR and restoring organized rhythm.

In the present paper we describe the use of an evolutionary algorithmic approach to solving the ablation problem. We sought to determine whether the evolved ablation-line distributions would be commensurate with the principles upon which the conceptually-guided strategy is founded. We postulated that if the precepts of our conceptual framework are correct then even an algorithmically derived ablation approach (which has no information about electrophysiologic principles) would nevertheless arrive at ablation lesion sets that adhere to the “rules” prescribed by the conceptually-guided strategy.

### **Basis for the conceptually guided strategy:**

Due to the refractory properties of myocytes, activation waves cannot simply reverse direction; therefore reentry requires a continuous activation path that comprises a circuit (closed loop) without which propagation ceases. This implies the vulnerability of all reentrant activity (MWR included); if its circuit(s) is interrupted, reentry terminates. When considered from this perspective the challenge for altering atrial substrate, so as to promote organized rhythm, is to identify an ablation-line distribution that has the maximum probability of interrupting the moving circuits of MWR.

We have previously demonstrated that 1) for a moving circuit, circuit interruption/annihilation occurs when the circuit-center collides with an outer boundary 2) the probability of spontaneous

termination correlates with the probability of such collisions and therefore is directly proportional to the total outer boundary length and inversely proportional to the tissue surface area 3) the probability of collision/termination can therefore be increased via creation of linear scars that extend the outer boundary, increasing the boundary-length to tissue-area ratio. 4) Finally, we demonstrated that in the setting of regional variation of circuit density, ablation lines are more effective when placed in areas with higher circuit density (Spector 2012).

## **Methods:**

### **Experimental design**

We used a covariance matrix adaptation evolutionary strategy (CMA-ES) (Hansen and Ostermeier 2001) to evolve the “fittest” distribution (location, orientation and length) of six linear scars. Fitness feedback was based upon the extent to which these ablation lines decreased the ability to induce and sustain MWR in each tissue tested. We assessed the characteristics of the evolving ablation lesion sets with regard to their adherence to the principles outlined by the conceptual strategy, specifically: 1) the percent of lines that are contiguous with the tissue’s outer boundary and 2) the total contiguous tissue area (i.e. the amount of tissue not electrically isolated (quarantined) by enclosing ablation lesions). Additionally, in order to test whether the CMA-ES would identify the strategy of concentrating ablation lines in regions of higher circuit density, we evolved ablation lines under two conditions: 1) “homogeneous” simulated tissue in which circuits were uniformly distributed (control) and 2) “heterogeneous” simulated tissue containing a patch that had a higher concentration of circuits than the remainder of the tissue (Figure 1). We then measured the density of ablation lines within the high circuit density patch compared with the same tissue region in the control.

### **Computational model of electrically excitable tissue:**

#### *Model design*

We used a computational model of electrically excitable tissue that is a hybrid between a physics-based and a cellular automaton model, described previously (Spector, Habel et al. 2011). Briefly, tissue is comprised of a flat two dimensional grid of “cells” representing a large number of myocytes.

#### *Excitation*

Each cell can be in an excited, refractory or quiescent state. When excited the cell’s voltage changes in a specified sequence (an action potential (AP)). Upon excitation the cell’s voltage abruptly increases (depolarization) over an activation period,  $T_a$ . This is followed by a plateau period,  $T_p$ . Next there is a linear reduction in voltage to baseline (repolarization) over a period,  $T_r$ . At baseline cells are in the quiescent state (excitable) with zero voltage. If their voltage is increased above the activation threshold,  $V_{thr}$ , the cell moves to the excited state and an AP ensues. Once excited the cell is refractory to re-excitation until its voltage decreases below  $V_{thr}$ ; therefore following activation, the time required to repolarize back below threshold, the action potential duration (APD), determines

the refractory period of the cell. The rate of depolarization is variable and emergent, decreasing inversely with the minimum voltage reached at the time of re-excitation,  $V_{\text{trough}}$ . The rate of repolarization is also dynamic and emergent, varying with the time from repolarization to subsequent excitation (the diastolic interval). The result of these dynamic parameters is excitation-rate dependent depolarization velocity and APD conferring conduction velocity and refractory period restitution, respectively.

### *Propagation*

Cells are connected by electrical resistors; current can flow between neighboring cells according to Ohm's law:  $V = IR$  where  $V$  is the intercellular voltage gradient,  $I$  is the intercellular current and  $R$  is the intercellular resistance. The cell capacitance is nominally set to 1 farad; therefore, there is a 1:1 relationship between change in current and in voltage.

This model design is sufficient to capture the functional properties of propagation required to emergently produce multi-wavelet reentry. These include source sink requirements for propagation and rate dependent variation of tissue excitability and refractoriness (restitution). In the presence of source sink determined propagation, conduction velocity (and failure) is dependent upon wave curvature. Under these circumstances spiral-waves of excitation can form at the edge of a curved wave-front; curvature-based conduction failure at the wave end creates a core of unexcited tissue around which rotation occurs.

### *Tissue parameters*

Simulated tissues used were comprised of a  $60 \times 60$  array of "cells". Each cell represents a large number of myocytes. The intercellular resistance was uniform in each direction and throughout the "homogeneous" tissue with an exception for the "heterogeneous" tissue explained below. The APD of each cell varied randomly throughout the tissue with a mean of  $100 \pm 25$ ms. In "homogeneous" tissue the distribution of baseline APD (prior to the effects of restitution) was randomly selected producing a relatively uniform concentration of circuits across the tissue following induction of MWR. In "heterogeneous" tissue the APD of cells within a patch of tissue ( $20 \times 20$  cells located along the middle third of the tissue border) was set to vary about a mean of  $50 \pm 25$ ms. The intercellular resistance within this patch was increased by 40% relative to the tissue outside the patch. In each case (homogeneous, heterogeneous) 10 separate replicates of macroscopically similar tissues were generated which had unique (random) distributions of APD (using the same mean and standard deviation).

### *Induction of multi-wavelet reentry*

MWR was generated using cross field stimulation. In the baseline state the duration of induced MWR is assessed, if termination occurred within the 2.5 second simulation the tissue was rejected and a new tissue generated. This process was repeated until 10 acceptable test tissues were generated.

### *Calculation of circuit density*

Using space-time plots of tissue voltage, the leading edge of each activation wave-front was defined as the sites of highest spatial derivative. The ends of each wave-front were then identified as those sites with only one neighbor on the wave-front's leading edge. Wave-end spatial density was then calculated over the entire space-time plot.

## **Evolutionary Strategy**

### *General description*

We used a powerful and mathematically-principled method called Covariance Matrix Adaptation Evolutionary Strategy (CMA-ES) that is designed to optimize functions of real-valued vectors. For example one might seek a real-valued vector  $\mathbf{z}$  that minimizes  $y$  in the fitness function  $f$ :

$$f(z_1, z_2, \dots, z_n) = y \quad (1)$$

The fitness function may be non-differentiable, non-linear and non-convex; CMA-ES treats the function as a black box. In our case  $\mathbf{z}$  corresponds to a set of ablation lines and  $f$  is a fitness function designed to optimize the ability of those lines to terminate and preclude MWR.

CMA-ES works by naturally following the contours of a co-evolving estimate of the surrounding fitness landscape in seeking to improve a single current solution estimate. Rather than maintaining a fixed population size as in many evolutionary algorithms, CMA-ES starts by assuming a multivariate normal distribution around a single randomly selected solution vector  $\mathbf{m}$  with covariance  $C$ , which is initially assumed to be a diagonal matrix (i.e., uncorrelated variables in solution space) with a pre-defined global standard deviation  $\sigma$ . It then proceeds to co-evolve improved estimates of the solution (new mean  $\mathbf{m}$ ) and an improved estimate of the covariance matrix  $C$  of the variables in surrounding solution space, as follows.

For every generation 1) a population cloud of  $\lambda$  potential solutions is generated according to the current estimate of the multivariate normal distribution described by  $C$  around the solution vector  $\mathbf{m}$ , 2) this population is then truncated to the best  $\mu$  solutions, where  $\mu$  is typically on the order of one half  $\lambda$ , 3) a fitness-weighted average of the remaining  $\mu$  solutions becomes the new  $\mathbf{m}$  (thus reducing the population to only 1 candidate solution), 4) the covariance matrix  $C$  is updated using local fitness landscape information based on the generational change in  $\mathbf{m}$  (a rank 1 update), the most recent  $\mu$  samples of the solution space in the vicinity of  $\mathbf{m}$  (a rank  $\mu$  update), and the length of evolution path of successive estimates of  $\mathbf{m}$ . As the search nears an optimum, the variance estimates approach zero and CMA-ES converges. Multiple random restarts of CMA-ES can be used to avoid getting stuck in local optima. To apply CMA-ES one must define an encoding for the solutions and a function to measure fitness.

### *Solution Encoding*

The encoding defines how a real vector  $\mathbf{z}$  maps to a solution, in this case a set of six ablation lines. Ablation lines are represented by a vector of 24 real numbers bounded from  $[-1; 1]$ .

$$\mathbf{z} = [x_1, y_1, x_2, y_2, \dots, x_{12}, y_{12}] \quad (2)$$

The successive pairs of values are interpreted as  $(x, y)$  Cartesian coordinates. Each coordinate pair defines the endpoints of a single straight ablation line, so there are six lines for each ablation set. Any cell  $i$  that falls underneath an ablation line is set to “dead” (unexcitable) and has an infinite resistance with its neighbors. All potential solutions ( $m$  and the clouds of  $\lambda$  potential solutions created each generation) are of this form.

We explicitly biased the initial ablation sets to discourage connections of ablation lines to an exterior boundary, in order to see if such connections would reliably evolve. All values in the initial vector  $m$  that encodes ablation sets are drawn from a uniform distribution  $[-0.4, 0.4]$ . The initial standard deviation  $\sigma$  is 0.2, hence the initial covariance matrix estimate is:

$$C = \begin{bmatrix} \sigma^2 & 0 & 0 \\ 0 & \ddots & 0 \\ 0 & 0 & \sigma^2 \end{bmatrix} \quad (3)$$

or  $\sigma^2\mathbf{I}$ . These parameters ensure that 95% of the ablation lines in the initial population are within the range of  $[-0.8, 0.8]$ ; thus, they tend not to connect to an exterior boundary.

### *Fitness function*

Tissue activation frequency ( $FR$ ) is defined as the mean activation frequency of all the cells:

$$FR = \frac{1}{TN} \sum_{i=1}^N s_i \quad (4)$$

where  $s_i$  is the number of activations of the  $i$ th cell,  $N$  is the total number of cells, and  $T$  is the number of seconds the tissue is simulated (2.5). The units of  $FR$  are activations per second. An  $FR$  of 1 means cells on average are activated once per second.

Our CMA-ES minimizes the fitness function:

$$f(\mathbf{z}) = F = \frac{1}{10} \sum_{j=1}^N FR_j \quad (5)$$

where  $F$  is the mean activation frequency  $FR$  of ten training tissues. Two constraints are imposed on the ablation sets: 1) The total number of ablated cells cannot exceed 18% of the tissue and 2) no more than 20% of the tissue can be quarantined. Any ablation set that violates these constraints is eliminated and replaced until an ablation set that satisfies the constraints is produced.

### *CMA-ES parameters*

Using the heuristic provided in [1], we selected population sizes of  $\lambda = 15$  and  $\mu = 7$  based on the genome size of 24. The CMA-ES was run for 200 generations (before which the rate of fitness improvement had diminished). For each evolutionary run, fitness was evaluated on ten randomly generated training tissues of a given type (homogeneous or heterogeneous) exhibiting MWR, and the resulting fitness values were averaged. By testing on 10 different tissues with varied distribution of similar electrophysiologic parameters the evolved solutions were general to a “type” of tissue rather than a specific individual tissue.

### **Lesion-set Characteristics**

#### *Percent of lesions contiguous with the outer boundary*

Let  $pC$  be the proportion of ablated cells that connect to a tissue boundary. If all ablated cells ultimately connect to a boundary,  $pC = 1$ . If the ablated cells form an island never connecting to an edge, then  $pC = 0$ .

#### *Percent quarantine*

If ablation lines enclose a region of the tissue, the enclosed cells become electrically isolated from the remainder of the tissue, effectively reducing the tissue area.  $pQ$  is defined as the proportion of cells isolated by ablation. If a tissue were ablated with a line extending from the top center of the tissue to the bottom center then  $pQ$  would equal 0.5.

#### *Boundary length to tissue area*

Let  $pA$  be the proportion of cells that are ablated. The length of the exterior boundary  $L$  is the total number of ablated cells connected to the exterior boundary ( $N pA pC$ ) plus the exterior boundary ( $B$ ) (which is  $240 = 60 \times 4$  for a  $60 \times 60$  tissue bounded on its four sides). The contiguous electrically excitable tissue area  $A$  is the total number of cells  $N$  minus the ablated cells,  $pA$ , and the quarantined cells,  $pQ$ . To test our hypothesis that the probability of MWR termination is directly proportional to the exterior boundary length and inversely proportional to the tissue surface area, we calculated the ratio:

$$\frac{L}{A} = \frac{N \cdot pA \cdot pC + B}{N(1 - pA - pQ)} \quad (6)$$

#### *Ablation line concentration*

We are interested in the relative amount of ablation lines for some subset or patch of the tissue. The ablation line concentration for a patch of  $M$  cells is the proportion of ablated cells inside the patch.

$$\frac{1}{M} \sum_j^M \begin{cases} 1, & \text{cell } j \text{ is ablated} \\ 0, & \text{cell } j \text{ is not ablated} \end{cases} \quad (7)$$



This measurement will recover the total proportion of cells that are ablated ( $p_A$ ) if  $M$  equals  $N$ .

### **Testing the Fitness Advantage of Boundary-Continuity**

To determine the contribution of boundary continuity to the fitness of each final evolved set of ablation lines we retested their fitness after disconnecting them from the tissue edge. The last two ablation lesions (points) connecting the line to the tissue boundary are “un-ablated” so that no ablation lines connect to the exterior boundary and  $p_C = 0$ .

### **Protocols**

We ran two sets of experiments with ten independent evolutions each. In the first set we evolved ablation lesion sets on homogeneous tissues (described above). In the second we evolved ablation lesion sets on tissue containing a patch of cells with shorter wave length (refractory period  $\times$  conduction velocity) due to reduced APD and increased intercellular resistance. In the latter tissues we confirmed that there was increased circuit density in the short wave-length patch (**Figure 1**).

### **Results:**

In the first set of experiments we examined the proportion of ablation lines contiguous with the exterior boundary ( $p_C$ ), the amount of quarantined tissue ( $p_Q$ ), and the length to area ratio ( $L/A$ ) (the total exterior boundary length, including ablation lines divided by the contiguous tissue area excluding quarantined tissue) and the fitness (FR). The results (mean  $\pm$  standard error of the mean (SEM)) are presented in figure 2. Fitness improves (i.e. the activation frequency (FR) decreases) as lesions evolve ( $0.93 \pm 0.04$  to  $0.08 \pm 0.00$   $p < 0.001$  according to Student's t-test). The proportion of ablation points contiguous with the exterior boundary ( $p_C$ ) steadily increases ( $0.01 \pm 0.01$  to  $0.99 \pm 0.01$ ,  $p < 0.001$ ). The proportion of ablated cells (both contiguous and non-contiguous) with respect to the whole tissue also increases ( $0.03 \pm 0.00$  to  $0.09 \pm 0.00$ ,  $p < 0.001$ ). The proportion of quarantined tissue also increases ( $0.00 \pm 0.00$  to  $0.15 \pm 0.01$ ,  $p < 0.001$ ). The net result is an increase in the length to area ratio ( $0.07 \pm 0.00$  to  $0.20 \pm 0.00$ ,  $p < 0.001$ ).

### **Fitness Advantage of Boundary-Continuity**

As the total length of ablation lines contiguous with the exterior boundary ( $L$ ) decreases, we expect that ablation set to be less likely to terminate MWR. To test this hypothesis, in each of the best evolved ablation sets, the last two ablation points connecting a line to the tissue edge were “unablated” and fitness retested. Ten new test tissues (that were not used during training) exhibiting MWR were generated to re-evaluate each modified ablation set. Prior to modifying the ablation sets, the average  $p_A = 0.091 \pm 0.002$ , the average  $p_Q = 0.16 \pm 0.02$ , the average  $p_C = 0.99 \pm 0.02$ , the average  $L/A = 0.20 \pm 0.01$ , and the average probability to terminate MWR  $p_T = 0.90 \pm 0.03$  (mean  $\pm$  SEM). Following ablation modification (disconnection from outer boundaries), the average  $p_A = 0.089 \pm 0.002$ , the average  $p_Q = 0.08 \pm 0.02$ , the average  $p_C = 0.00 \pm 0.00$ , the average  $L/A = 0.08$

$\pm 0.00$ , and the average probability to terminate MWR  $pT = 0.23 \pm 0.04$ . Comparing between the two cases, all measurements are significantly different ( $p < 0.001$  for  $pC$ ,  $pT$ , and  $L/A$ ;  $p < 0.01$  for  $pQ$ ) except for the total proportion of ablations.

## High Circuit Density Patch

In a second set of experiments we examined the ablation sets that evolved in heterogeneous tissue (with a high circuit density patch). We compared the density of ablation lesions in the top middle portion of the tissue (high circuit density patch) with that in the remainder of the tissue. Ablation density was higher in the patch than in the remainder of the tissue ( $0.08 \pm 0.01$  vs  $0.15 \pm 0.01$ ,  $p < 0.001$  – figure 3a). In contrast, the ablation density was the same in and outside of the top middle portion of the tissue in the homogeneous tissue experiments (figure 3b).

## Discussion:

Based upon an explanatory model for propagation through excitable tissue we postulated that MWR necessitates complete circuits for its perpetuation. This implies the strategy for its ablation: interrupt these circuits causing termination. Interruption requires complete circuit transection thus the first tenet of the conceptually-guided strategy: lines must be contiguous with the tissue's exterior boundary and extend to the circuit-core. To corroborate this principle using the CMA-ES we purposely created a first generation of ablation lines that were not contiguous with an outer boundary so that if the evolved ablation strategies had a greater percentage of lines connected to the outer boundary than would result from random mutation, then fitness pressure for such connection must be at work. Starting from an initial generation in which virtually none of the lines were contiguous with the tissue's outer boundary (by design), by the end of evolution nearly 100% of lines were connected. By comparison, in a set of 10 randomly drawn ablation-line sets (each of the 24 elements were drawn from a uniform distribution over the entire domain  $[-1,1]$ ) only 27% of lines were contiguous with the tissue border.

To confirm that it was continuity with the boundary that conferred increased fitness, we eliminated the ends of each ablation line at its point of contact with the boundary. In each case the fitness and MWR termination efficacy decreased when lines were disconnected from the outer boundary.

If collision is fundamental to efficacy then lines in areas with higher circuit density, where collision is more likely, should be more effective than those in areas with lower density. To test whether fitness pressure would drive ablation lines toward areas of high circuit density, we evolved solutions on tissue with a patch of increased circuit density. In each evolution performed on heterogeneous tissue, ablation lines were concentrated within the high circuit-density patch. In contrast, the density of ablation lines in the same tissue region was not increased when evolved on homogeneous tissue.

The current results help to validate the fundamental principles that underlie the conceptually-guided strategy. The two approaches to searching the solution space of the ablation problem (evolutionary algorithmic and conceptually-guided) are fundamentally different and *non-derivative*. The fact that in each case the lesion sets adhere to the same principles (due to fitness pressure on the one hand and by mechanistically-inspired design on the other) supports the importance of these tenets. This is critical because in human hearts we are unable to apply an evolutionary approach (we must deliver a single lesion set). The key characteristic of the conceptually-guided approach is that it effectively allows for *a priori* efficacy evaluation (through mental modeling) so when ablation lesions are delivered they have already been “tested”.

### **Comparing evolutionary and conceptually-guided methods for searching large solution spaces:**

#### *The solution space*

In modern science there has been a growing appreciation of the existence and nature of complex systems. Such systems, comprised of multiple parts interacting in non-linear fashion, are capable of extremely complex behaviors. The heart is such a system. It has a very simple job description: it must pump blood. The achievement of this task, however, is tremendously complex requiring the coordinated activity of billions of ion channels in millions of cells interacting electrically and mechanically in an elegant symphony, and without the benefit of a conductor. When functioning normally the heart sustains life; when sufficiently deranged it precludes it.

In the context of MWR, ablation amounts to manipulating the structure of a complex non-linear system so as to constrain its behavior. Even if we limit allowable manipulations to the placement of ablation lines, the number of possible solutions is vast and exhaustive search is intractable.

#### *The search strategies*

Thus, a critical question is: “How can one most efficiently search the solution space of the ablation problem?” In this paper we compare the results of two very different approaches to addressing this problem – an evolutionary algorithmic approach and a conceptually-guided approach.

These two are fundamentally and profoundly different strategies. The former is a black box search that utilizes absolutely no information about the existence or mechanisms of cardiac electrical activity. Rather, the effectiveness of each generated potential solution is assessed and the potential solutions are perturbed and iterated with positive feedback in order to evolve progressively more effective solutions. The conceptually-guided approach is extremely different. It is a two-step process: 1) based upon preliminary observations of the system (tissue excitation) explanatory models for its behavior are postulated, these are tested by experiments, the results of which are used to iteratively improve the explanatory model. 2) The resultant model is then used *to guide the search* of the (ablation-problem) solution space.

In an elegant demonstration of the effectiveness of evolution's creative powers, one must note that it was an evolutionary search (Evolution) that produced both the tool (the brain) and the process (explanatory modeling) of conceptual-guidance as a search strategy.

### *Systematic Biases*

The conceptually guided strategy attempts to achieve a more efficient search of the vast solution space by examining only those solutions that are commensurate with the explanatory model on which it is based. This provides the efficiency of avoiding tests of "obviously" inadequate candidate solutions. This efficiency results from a systematic bias towards those candidates deemed likely to succeed. The bias however also systematically precludes identification/testing of "counter-intuitive" candidates. The evolutionary strategy is, however, blind to, independent of and hence unbiased by, the mechanisms by which its candidate solutions achieve their fitness. Evolutionary strategies therefore *do* have the potential to identify counter-intuitive solutions. But, evolutionary algorithms are also systematically biased (e.g. by virtue of the specific search method chosen, the fitness function used, and the solution encoding employed).

We attempted to compensate for the liability of the conceptually guided strategy's systematic biases by purposely biasing the CMA-ES *against* some of the design principles of the conceptual strategy; thus enhancing our confidence if it nonetheless selected candidate solutions with the same properties. The initial candidate ablation-lines were precluded from connecting to the tissue edge and based upon the ablation line encoding were biased against developing edge connection<sup>1</sup>. Similarly, the initial lines included virtually no quarantined area and were constrained to allow a maximum of 18% quarantine. Despite these restrictions nearly 100% of lines were connected to the tissue boundary and the percent quarantined achieved the allowable limit. Finally ablation-line concentration in a specific region was statistically unlikely (and was absent in homogeneous tissue) but in the presence of a patch with high circuit density lesions nonetheless concentrated in the patch.

### **Conclusions:**

Despite the fact that our evolutionary strategy was blind to the mechanisms (and existence) of cardiac propagation, it evolved ablation lesions that adhered to the guiding principles set forth by our mechanistically inspired approach to the ablation of MWR. This finding lends support to the validity of these principles which suggest that ablation of MWR in humans should be guided by the density of circuits and comprised of linear lesions contiguous with the atria's electrical boundaries.

### **Limitations:**

This work explores ablation of MWR in a virtual arena and hence the applicability of the findings is relevant to human MWR only to the extent that the assumptions of the model accurately reflect the

---

<sup>1</sup> During evolution ablation endpoint coordinates were selected from the tissue matrix; because there are a greater number of interior coordinates than boundary coordinates the likelihood of evolving lines connected to the edge was lower than that of evolving lines disconnected from the edge.

functional behavior of cardiac rhythms. In order for this work to be extended into humans it will require validation in a biologic system.

## Acknowledgments:

## References:

- Calkins, H., K. H. Kuck, et al. "2012 HRS/EHRA/ECAS Expert Consensus Statement on Catheter and Surgical Ablation of Atrial Fibrillation: Recommendations for Patient Selection, Procedural Techniques, Patient Management and Follow-up, Definitions, Endpoints, and Research Trial Design: A report of the Heart Rhythm Society (HRS) Task Force on Catheter and Surgical Ablation of Atrial Fibrillation. Developed in partnership with the European Heart Rhythm Association (EHRA), a registered branch of the European Society of Cardiology (ESC) and the European Cardiac Arrhythmia Society (ECAS); and in collaboration with the American College of Cardiology (ACC), American Heart Association (AHA), the Asia Pacific Heart Rhythm Society (APHRS), and the Society of Thoracic Surgeons (STS). Endorsed by the governing bodies of the American College of Cardiology Foundation, the American Heart Association, the European Cardiac Arrhythmia Society, the European Heart Rhythm Association, the Society of Thoracic Surgeons, the Asia Pacific Heart Rhythm Society, and the Heart Rhythm Society." *Heart Rhythm*.
- Calkins, H., M. R. Reynolds, et al. (2009). "Treatment of Atrial Fibrillation With Antiarrhythmic Drugs or Radiofrequency Ablation: Two Systematic Literature Reviews and Meta-Analyses." *Circ Arrhythmia Electrophysiol* **2**(4): 349-361.
- Hansen, N. and A. Ostermeier (2001). "Completely derandomized self-adaptation in evolution strategies." *Evol Comput* **9**(2): 159-195.
- Jais, P., M. Hocini, et al. (2004). "Technique and results of linear ablation at the mitral isthmus." *Circulation* **110**(19): 2996-3002.
- Moe, G. K. and J. A. Abildskov (1959). "Atrial fibrillation as a self-sustaining arrhythmia independent of focal discharge." *Am Heart J* **58**(1): 59-70.
- Spector, P. S., Correa de Sa, Daniel D., Tischler, Ethan, Thompson, Nathaniel, Habel, Nicole, Stinnett-Donnelly, Justin, Benson, Bryce E., Bates, Jason H.T. (2012). "Ablation of Multi-Wavelet Reentry: General Principles and In Silico Analyses." *Europace*(In review).
- Spector, P. S., N. Habel, et al. (2011). "Emergence of complex behavior: an interactive model of cardiac excitation provides a powerful tool for understanding electric propagation." *Circulation: Arrhythmia and Electrophysiology* **4**(4): 586-591.

## Figures:

FIG1.pdf in color for print and web

**Figure 1: Circuit Density Maps** - a) Homogeneous tissue without a short wave-length patch, b) Heterogeneous tissue with a short wave-length patch. Note the increased circuit density in the top middle of panel b at the site of the short wave-length patch.

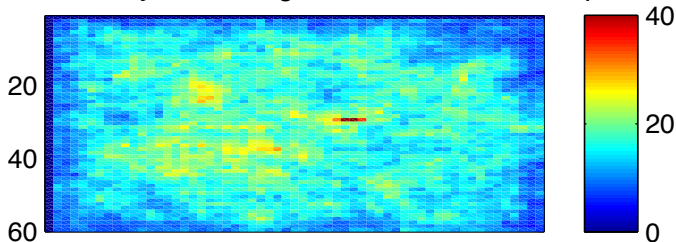
FIG2.pdf in color for print and web

**Figure 2: Ablation Lesion Characteristics and Fitness** - tissue with homogeneous circuit density. Note that  $pC$  and  $pQ$  (and therefore  $L/A$ ) increase during evolution as fitness improves.

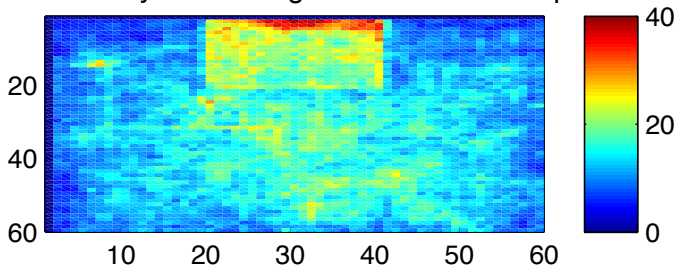
FIG3.pdf in color for print and web

**Figure 3: Ablation Density vs. Circuit Density** - Tissue without (a) and with (b) a high circuit density patch. Ablation density is markedly increased in the high circuit density region.

**Figure 1:** (a) Circuit density for homogeneous tissue without patch



(b) Circuit density for heterogeneous tissue with patch



proportion

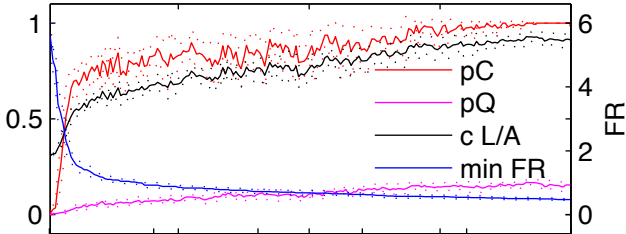
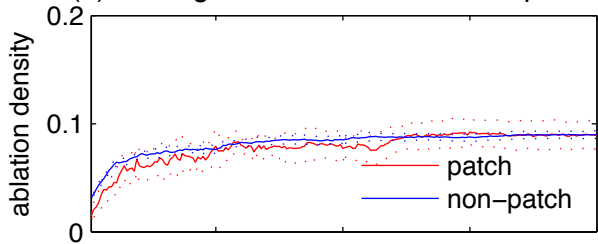


**Figure 3**

(a) Homogeneous tissue without a patch



(b) Heterogeneous tissue with a patch

